J Biomol NMR (2014) 59:161–173
DOI 10.1007/s10858-014-9836-0

ARTICLE

Aliphatic chain length by isotropic mixing (ALCHIM): determining composition of complex lipid samples by ^{1}H NMR spectroscopy

Joseph R. Sachleben · Ruiyang Yi · Paul A. Volden · Suzanne D. Conzen

Received: 24 February 2014 / Accepted: 2 May 2014 / Published online: 15 May 2014

Abstract Quantifying the amounts and types of lipids present in mixtures is important in fields as diverse as medicine, food science, and biochemistry. Nuclear magnetic resonance (NMR) spectroscopy can quantify the total amounts of saturated and unsaturated fatty acids in mixtures, but identifying the length of saturated fatty acid or the position of unsaturation by NMR is a daunting challenge. We have developed an NMR technique, aliphatic chain length by isotropic mixing, to address this problem. Using a selective total correlation spectroscopy technique to excite and transfer magnetization from a resolved resonance, we demonstrate that the time dependence of this transfer to another resolved site depends linearly on the number of aliphatic carbons separating the two sites. This technique is applied to complex natural mixtures allowing the identification and quantification of the constituent fatty acids. The method has been applied to whole adipocytes demonstrating that it will be of great use in studies of whole tissues.

Keywords Fats · Lipids · Metabolomics · Lipidomics · Food science · NMR · TOCSY

Electronic supplementary material The online version of this article (doi:10.1007/s10858-014-9836-0) contains supplementary material, which is available to authorized users.

J. R. Sachleben (✉) · R. Yi
Biomolecular NMR Core Facility, Biological Sciences Division, The University of Chicago, Chicago, IL 60637, USA
e-mail: jsachleben@uchicago.edu

P. A. Volden · S. D. Conzen
Department of Medicine, The University of Chicago, Chicago, IL 60637, USA

Introduction

Understanding the composition of mixtures of lipids is important in diverse areas of research including medicine, food science, and biochemistry. Lipidomics is a growing area of interest in the biomedical community as lipid misregulation has multiple roles in human disease. For instance, the relationship between atherosclerosis and dietary lipids stems from observations made by Rudolph Virchow in the nineteenth century, and remains central in the study of atherogenesis today (Watson 2006; Merched and Chan 2013; Rasmiena et al. 2013; Didangelos et al. 2012; Kontush and Chapman 2010; Camont et al. 2013). Dietary lipids, lipid metabolism, and cellular lipid composition also play obvious and direct roles in the pathogenesis of the cluster of disorders that include obesity, type 2 diabetes, and the dysmetabolic syndrome (Gonzalez-Covarrubias 2013; Boslem et al. 2013; Kien et al. 2013; Ståhlman et al. 2012; Meikle and Christopher 2011; Gross and Han 2007; Kwan et al. 2013). Importantly, all of these roles are heavily influenced by lipid composition, in particular the length of lipid chains and their degree of saturation. Interestingly, some cancer cells, which characteristically undergo high rates of cell division, scavenge lipids of specific length and saturation for structural roles, but also to aid in survival during hypoxia (Kamphorst et al. 2013). Many lipids have important endocrine roles that depend on structural aspects, including length and degree of saturation. For example, polyunsaturated fatty acids (PUFAs) are precursors for the hormone-like eicosanoids including prostaglandins, leucotrienes, and thromboxanes (O'Donnell et al. 2009). Furthermore, saturated fatty acids have been associated with insulin resistance, whereas PUFAs have been associated with increased insulin sensitivity (Fedor and Kelley 2009; Riccardi et al.

2004). The ratio of dietary and adipose tissue ω-3/ω-6 fatty acids has been associated with poor outcomes in breast cancer (Simonsen et al. 1998; Thiebaut et al. 2009). Because of all these relationships between the type of fatty acid and health, food scientists have long studied the fatty acid composition of foods. These studies have ranged from the common [cow milk (Casado et al. 2009)] to the exotic [recent analyses of camel (Sbihi et al. 2013) and goat (Longobardi et al. 2012) meat] as well as the oxidation of edible oils upon heating (Guillén and Ruiz 2001).

Standard lipidomic analyses utilize powerful mass spectrometric (MS) techniques, which usually require covalent modification of lipids, such as esterification. For example, in the standard AOAC method (969.33 and 963.22 F) for the analysis of glycerides and phospholipids, glycerolipids are first saponified in methanolic NaOH solution and then methyl esterified in the presence of BF_3. Gas chromatography (GC) analyzes the resulting methyl esters. This method is limited by interference if large fractions of unhydrolyzable compounds are present and due to chemical alteration of modified fats, such as aldehydes, ketones, and conjugated polyunsaturated materials (AOAC 1995). These methods, though clearly instrumental in providing data on lipid composition, have shortcomings, the most apparent being that they cannot be used on samples in intact tissues or cells. Another complication of MS-based techniques is that time courses can be followed only in parallel samples, which are prone to usual biological variability.

An NMR-based technique will complement MS-based techniques, and allow application of lipidomics to intact cells and tissues. Furthermore, this will facilitate following a single cell type or tissue over a time course. In addition, H NMR avoids the above-mentioned complications by allowing analysis with little chemical modification, typically extraction and dissolution in deuterated chloroform. In this paper, we present a new NMR-based lipidomic technique, aliphatic chain length by isotropic mixing (ALCHIM), to address these problems.

Previously, it has been shown that simple 1D ^{1}H NMR spectra can provide information on the relative quantities of saturated and unsaturated fatty acids, average molecular mass, the average number of double bonds, the presence of modified fats, and some acyl group identification (Guillén and Ruiz 2001). Figure 1a shows the ^{1}H 1D spectra of three saturated fatty acids. The spectra are very similar with only the shape of the polymethylene peak at 1.3 ppm changing in the different fatty acids. Relative integrals can identify pure saturated fatty acids, but such an approach will fail in mixtures. Similar overlap occurs in unsaturated and modified fatty acids of differing lengths.

New methods need to be developed to simply and accurately characterize these important samples. We present a method based on the TOCSY experiment (Braunschweiler and Ernst 1983), which correlates all members of the spin system by an isotropic mixing period (Rule and Hitchens 2006). Van and Shaka (1998) have measured the selective TOCSY spectrum in 1-dodecanol demonstrating that transfer down long aliphatic chains is possible. While a 2D-TOCSY spectrum as typically applied is not very useful on lipid samples as the assignment is already established, the mixing period dependence of the magnetization transfer among the resolved peaks in lipids will measure the number of carbons separating those sites. As we will show below, ALCHIM uses the isotropic mixing time dependence of magnetization transfer to allow the identification of saturated fatty acids and the position of modification in unsaturated and other modified fatty acids. In addition, it permits the quantification of mixtures of fatty acids. We show applications to biological and biomedical samples.

Materials and methods

Sample preparation

Pure fatty acids samples were purchased from Sigma-Aldrich and used without further purification. Analytical standard coconut oil and fatty acid methyl ester reference mixture 2 (FAME-RM2) were supplied by Supelco (Lot No: LB89794V and LC02665, respectively) Certificates of analysis are provided in Online Resource 1.

Samples from mouse adipose tissue were prepared by the following method. Gonadal adipose tissue was harvested from 16 week old female CD-1 mice. Upon harvest, adipose tissue was placed into a microcentrifuge tube containing DMEM high glucose media with 1 % pen/strep. The tissue was then finely minced, spun at 100*g* for 30 s, and the floating layer enriched in adipocytes was then transferred to a new pre-weighed tube. 3 mL of DMEM high, 1 % P/S media with 2 mg/mL collagenase type I (Worthington Biochemical) media was added, per gram adipose tissue, to the new tube. The collagenase digestion continued for 30 min, shaking at 37 °C. The tube was then spun at 100*g* for 1 min and the floating adipocytes were filtered through a 350 μm nylon mesh. The remaining media was removed from beneath adipocytes with a needle and syringe. As described below, either intact adipocytes were used or lipids were extracted from adipocytes for NMR studies.

Lipids were extracted from the adipocytes using the Folch method. Briefly, 1 mL of methanol was added to 100 μL of adipocytes. The adipocytes were then sonicated for 10 s at 6 W. The entire volume was transferred to a Pyrex tube with Teflon cap, 2 mL of chloroform was added

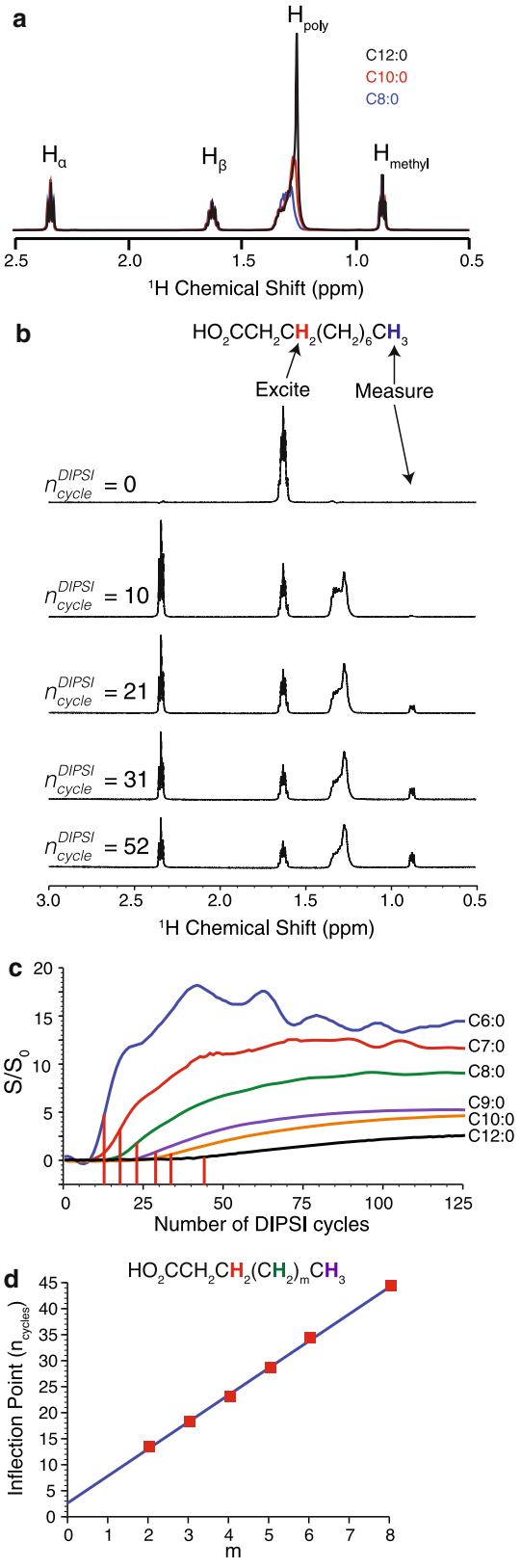

◀**Fig. 1** The ALCHIM Experiment. **a** ^{1}H NMR of octanoic (C8:0), decanoic (C10:0), and dodecanoic acids (C12:0). **b** Selective TOCSY spectra of decanoic acid. The H_β are initially excited and spectra are measured as a function of the number of DIPSI cycles applied. **c** Integral of methyl peak as a function of the number of DIPSI mixing cycles for C6:0 to C12:0 saturated fatty acids. Integrals are plotted in percent and are normalized to the integral of the excited H_β peak. *Vertical bars* indicate first inflection point. **d** Plot of the first inflection point as a function of the number of carbons separating the H_β and H_{methyl}

to the tube, then the contents was allowed to shake and incubate at ambient temperatures. Following addition of 850 µL water and mixing, tubes sat for 10 min and then the lower phase was recovered. The upper phase was washed with 1.5 mL 86:14.1:1, $CHCl_3$/methanol/water, v/v/v solvent mix and the lower phase was recovered and combined with the first recovery. To extract neutral lipids, the solvent was evaporated under nitrogen gas and lipids were resuspended in 100 µL of $CHCl_3$. The solution was then added to a cyanopropyl solid phase extraction column (Fisher AT209550) that has been pre-rinsed with 10 mL of hexane: ether:acetic acid, 80:20:1. Neutral lipids were eluted and collected off the column with a second 10 mL volume of hexane: ether: acetic acid then evaporated under nitrogen and stored at −80 °C until use.

NMR experiments

All pure fatty acid solutions were prepared at a concentration of 5 mg of fatty acid per 1 mL of $CDCl_3$/0.05 % TMS. Extracted lipids were dissolved in $CDCl_3$/0.05 % TMS. All ^{1}H NMR spectra were acquired on a 600 MHz Bruker AVANCE IIIHD NMR spectrometer operating at a spectrometer frequency of 600.13 MHz using a room temperature inverse triple resonance probe tuned to ^{1}H, ^{15}N, and ^{13}C. ^{1}H 1D spectra were acquired with a 1.14 s acquisition time, 1.5 s recycle delay, 8 scans, and 90° pulse length of 7.8 µs over a sweep width of 8.00 ppm with the spectrum centered at 3.00 ppm. The low power ^{1}H 90° pulse length used in the DIPSI-II sequence was 26 µs.

Isotropic mixing in total correlation spectroscopy (TOCSY) transfers in-phase magnetization along an entire spin system (Ernst et al. 1990). Online resource figure 1 shows the selective TOCSY sequence, Bruker's seldigpzs sequence (Online Resource 1), where a selective Hahn echo refocuses only the selected spin, which is then transferred down the fatty acid chain by the DIPSI-II isotropic mixing sequence (Kessler et al. 1986; Stonehouse et al. 1994; Stott et al. 1995). Initial and final zero-quantum

coherence is suppressed with simultaneous gradient and adiabatic 180° pulse (Thrippleton and Keeler 2003). A variable loop counter is used around the fixed period of the DIPSI sequence to make it a pseudo 2D experiment where the number of DIPSI cycles applied during the mixing time is varied. A typical DIPSI cycle was 2.993 ms. An ALCHIM transfer function is the DIPSI cycle dependence, n_{cycle}, of the integral of the detected resonance. This is typically normalized to the integral of the excited peak after a single DIPSI cycle, for which little magnetization transfer has occurred.

Theoretical calculation

ALCHIM transfer curves in fatty acids can be modeled as a chain of N spin ½ nuclei coupled only to their nearest neighbors where the first spin of the chain is excited while the last is detected. During the mixing period, the flip-flop terms of the isotropic Hamiltonian relay the magnetization down the spin chain until it arrives at the detection site. The isotropic Hamiltonian for such a system is

$$\mathscr{H} = 2\pi J \sum_{i=1}^{N-1} \vec{I}_i \cdot \vec{I}_{i+1}, \tag{1}$$

while the initial density matrix is

$$\rho(0) = I_{Z,1} \tag{2}$$

and the observable is

$$\mathscr{O} = I_{Z,N}. \tag{3}$$

In this model, the first spin is excited, the magnetization is transferred along the chain and only the magnetization on the last spin is detected. The signal on the detected spin as a function of n_{cycle}, i.e. the transfer function, is given by

$$\begin{aligned} S(n_{cycle}) &= Tr\left\{\mathscr{O} e^{-i\mathscr{H} n_{cycle} t_{cycle}} \rho(0) e^{i\mathscr{H} n_{cycle} t_{cycle}}\right\} \\ &= Tr\left\{I_{Z,N} e^{-i\mathscr{H} n_{cycle} t_{cycle}} I_{Z,1} e^{i\mathscr{H} n_{cycle} t_{cycle}}\right\} \\ &= a_0 + \sum_{i=1}^{N_{\max}} a_i \cos\left(\pi n_{cycle} \nu_i t_{cycle}\right) \end{aligned} \tag{4}$$

where t_{cycle} is the period of a single ideal isotropic mixing sequence cycle, and the ν_i are proportional to the J-couplings between the neighboring spins but they are typically not rational multiples of J in large systems. Calculations for linear chains of 2–7 spins are shown in the online resources and demonstrate that the transfer time across the chain increases linearly with the number of spins separating the excited and detected sites. (Online Resource 1 and 2) This suggests that we can use the transfer dynamics under isotropic mixing as a ruler of fat length. In addition, after a long period of isotropic mixing, a quasi-equilibrium state is expected which is given by

$$\rho_{QE} = \frac{1}{N}\sum_{i=1}^{N} I_{Z,i} = \frac{1}{N} I_Z^{Tot}, \tag{5}$$

i.e., the magnetization will be evenly distributed among all the protons of the lipid. The simulations show this effect, (Online Resource 2) which limits the sensitivity of this method in long chain, saturated fatty acids.

Data analysis

ALCHIM spectra were integrated in the Bruker Topspin software with careful baseline correction around each peak multiplet. The Topspin T1/T2 module then extracted the integrals as a function of n_{cycle} from the pseudo 2D dataset. Transfer functions of mixtures were modeled as a linear combination of constituent transfer functions,

$$S_{\text{model}}(n_{cycle}) = \sum_{i=1}^{n_{components}} f_i S_i(n_{cycle}). \tag{6}$$

The number of fatty acid components in the mixture is $n_{components}$ while their fraction is f_i. S_i's are the measured transfer functions of pure substances. A subset of components can be modeled as long as the number of DIPSI cycles is limited to less than the number necessary for longer components to contribute to the transfer function. Fatty acid fractions were extracted by calculating the posterior probability function (Sachleben 2006; Sivia 1996; Gelman et al. 2004) that the modeled fractions describe the measured transfer function up to the maximum number of DIPSI cycles used. The posterior probability function, P, is given by

$$P = \frac{N}{\sigma^{n_{cycle}^{\max}+2}} e^{-\frac{1}{2\sigma^2}\chi^2}, \tag{7}$$

where

$$\chi^2 = \sum_{n=1}^{n_{cycle}^{\max}} \left(S_{\exp}(n) - S_{\text{model}}(n)\right)^2, \tag{8}$$

σ is the rms noise on the measured transfer curve which was treated as an additional parameter in the posterior probability, and N is a normalization constant that ensures that the total probability sums to 1. P was calculated on a multidimensional grid depending upon the number of parameters being determined. Typically a large mesh grid over a fairly large range of fractions is initially searched and then refined to find the allowed range of parameters. The largest calculation performed was the final determination of the saturated fatty acids in coconut oil. In that case, the posterior probability was calculated on a 5 dimensional grid consisting of 31^4 points of the fractions of hexanoic, octanoic, decanoic, and dodecanoic acids, and 15 points on the noise. This was projected onto each of the

fraction axes for analysis and display. Notebooks written for Mathematica 9 and run on a MacBook Pro performed all calculations. More details of the Bayesian analysis of the data and an example Mathematica Notebook is provided in the online resources (Online Resources 2).

Results

ALCHIM in saturated fatty acids

Figure 1b shows DIPSI cycle dependence of the transfer of magnetization along the fatty acid chain in decanoic acid (C10:0) after excitation of the H_β. Integrals of the H_α, H_β, H_{PM}, and H_{methyl} are shown in Online Resources Figure 3. Initially, magnetization is transferred to the neighboring H_α and polymethylenes after only a couple of DIPSI cycles. The transfer between the H_α and H_β shows a damped oscillatory behavior because of the transfer between the neighboring protons and the loss of magnetization from this system as the magnetization is transferred into the polymethylenes. The oscillations in the integrals of H_α and H_β are anticorrelated: as magnetization is gained by H_α it is lost by H_β and vice versa. There is a significant lag in transfer to the terminal CH_3. Little magnetization has arrived at the CH_3 after 10 DIPSI cycles, but the peak is clearly visible after 21, Fig. 1b. Figure 1c shows the transfer curves of the series of saturated fatty acids from 6 to 12 carbons long. It is immediately obvious that the number of DIPSI cycles for magnetization transfer increases while the amount of magnetization transferred decreases as the length of the fatty acid chain grows. Figure 1d shows the first inflection point of the transfer curves in Fig. 1c as a function of the number of carbons separating the β and methyl protons. The first inflection point occurs when the rate of magnetization transfer to the detected location is maximal and provides a well-defined metric for quantifying transfer via isotropic mixing in a many-spin system, as opposed to the time for maximum transfer, which depends on the rate of magnetization transfer into and out of the detected site. Qualitatively, the first inflection point is expected to depend linearly on mixing time in these systems as each methylene has the same pattern of J-couplings responsible for magnetization transfer. The transfer through n methylenes requires n steps of transfer mediated by the same pattern of J-couplings. This linear relationship is borne out in both the theoretical calculations and the experiments on saturated fatty acid. From this, we can conclude that the ALCHIM experiment provides a convenient ruler of fatty acid length.

ALCHIM in mixtures of saturated fatty acids

Figure 2a shows the H_β to H_{methyl} transfer function for mixtures of hexanoic and octanoic acid from 0 to 100 % hexanoic acid. All the transfer functions for mixtures that contain hexanoic acid begin to increase after 10 DIPSI cycles while the pure octanoic requires 18. The intensity of the methyl peak between 10 and 18 cycles depends only on the presence of hexanoic acid. Beyond 18 cycles, octanoic acid begins to contribute. In addition, as the fraction of octanoic acid increases the limiting transfer decreases towards that of octanoic acid. These results suggest that the resulting transfer functions are linear combination of those for the pure substances; i.e.,

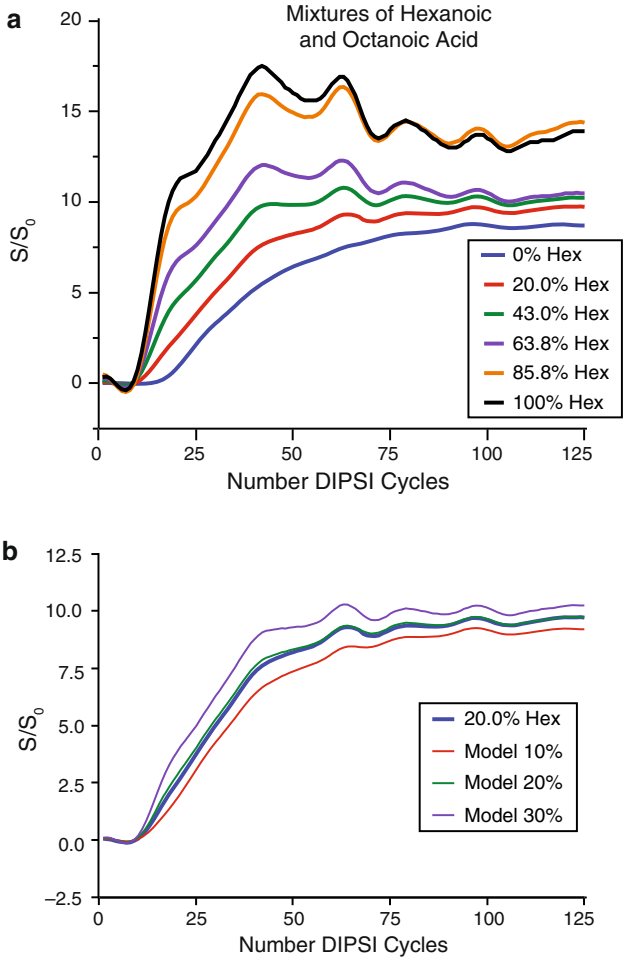

Fig. 2 **a** H_β to H_{methyl} transfer functions of mixtures of hexanoic and octanoic acid. **b** Transfer function for the 20 % hexanoic 80 % octanoic acid mixture as well as modeled transfer functions assuming 10, 20, and 30 % hexanoic acid

$$S(n\,\%\ \text{hexanoic}) = \frac{n}{100} S(100\,\%\,\text{hexanioc}) + \left(1 - \frac{n}{100}\right) S(100\,\%\ \text{octanoic}). \quad (9)$$

This modeling uses the experimentally determined transfer functions for the pure components with the only variable parameter being the fraction of hexanoic acid in the mixture. Figure 2b demonstrates that this model

successfully describes the data. The figure shows the 20 % hexanoic acid mixture with models calculated with Eq. 9 for 10, 20, and 30 % hexanonic acid. The 20 % model accurately predicts the data with 10 and 30 % being clearly distinct. From these simulations, it is clear that the composition fraction can be determined to a precision better than ±10 % in a binary mixture.

ALCHIM in unsaturated fatty acids

In addition to saturated fatty acids, ALCHIM can be applied to unsaturated fatty acids. Online Resource Figure 4 shows the spectra of oleic and linoleic acids. The allylic protons in oleic and palmitoleic overlap, while linoleic is at a higher shift. In unsaturated fatty acids, two transfer curves need to be measured: H_β to $H_{allylic}$ and H_{methyl} to $H_{allylic}$. Figure 3a shows the H_β to $H_{allylic}$ transfer functions of oleic, palmitoleic, and linoleic acids as well as the H_β to H_{methyl} for octanoic acid. These four transfer functions are essentially identical because the excitation and detection sites are each separated by four methylenes. Most interestingly is that the transfer function for the saturated octanoic acid detected at the methyl peak overlays with the unsaturated fatty acid transfer functions detected at the allylic site. This indicates that a ladder of transfer functions can be made from the saturated fatty acids for identifying the chain lengths in unsaturated fatty acids. Figure 3b demonstrates this on the H_{methyl} to $H_{allylic}$ transfer functions of oleic, palmitoleic, and linoleic acids. It is clear that 3, 4, and 6 carbons separate the methyl and allylic protons in linoleic, palmitoleic, and oleic acids, respectively. In PUFAs, transfer from the H_β and H_{methyl} to the $H_{vinylic}$ proton can also be followed. This transfer curve cannot be calibrated from the saturated fatty acids as the transfer across the unsaturated carbons occurs at a different rate from that of neighboring methylenes; however, the transfer function still depends upon the number of carbons separating the excitation and detection sites, Online Resource Figure 3b. ALCHIM experiments on polyunsaturated fatty acid standards can be run producing a database that can be compared to unknown samples.

ALCHIM in natural fat mixtures

Coconut oil

We further extend ALCHIM to natural mixtures of lipids. A sample of analytical standard coconut oil (Supelco) was purchased from Sigma-Aldrich and dissolved in deuterated chloroform. H_β to H_{methyl} and H_{methyl} to $H_{allylic}$ ALCHIM experiments were performed, Fig. 4. Figure 4a shows the H_β to H_{methyl} transfer function, which is sensitive to the saturated fatty acid components of the coconut oil. The measured transfer function does not follow any of the reference curves. This demonstrates that coconut oil contains a mixture of fatty acids. Since the transfer curve begins to significantly rise at the same number of cycles as octanoic acid, we can immediately conclude that octanoic acid is contained in coconut oil.

A more quantitative analysis of the transfer curve can be made by assuming that the observed transfer function is a linear combination of transfer functions of pure fatty acids. If we limit our analysis to the first 50 DIPSI cycles, we are sensitive only to hexanoic, octanoic, decanoic, and dodecanoic acids. The best-fit result is shown in red in Fig. 4a, while b shows the probability distributions of the

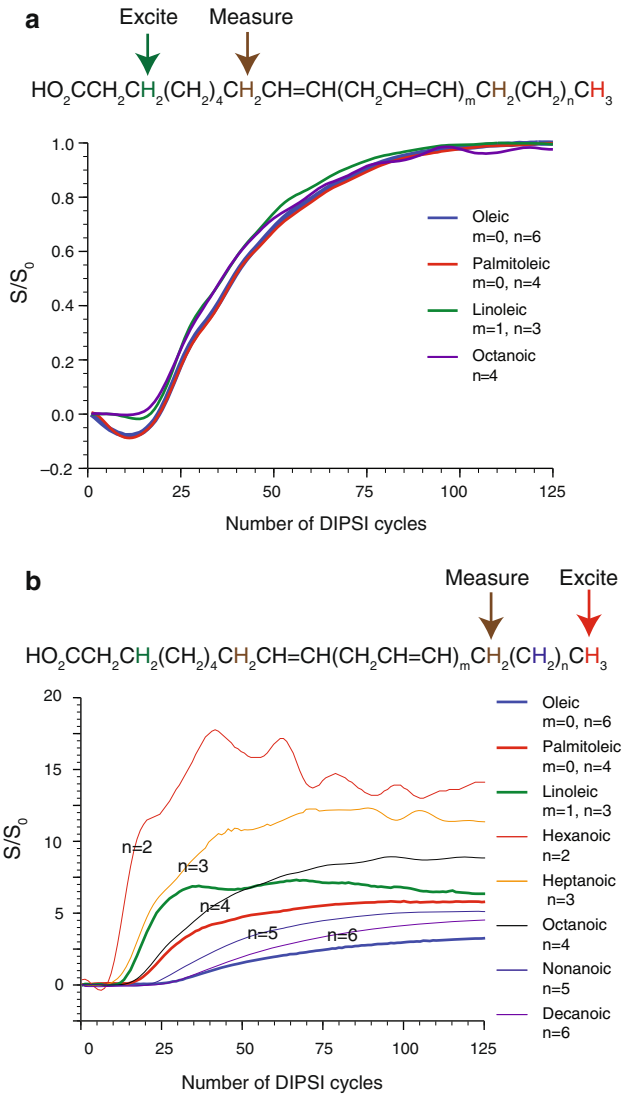

Fig. 3 **a** H_β to $H_{allylic}$ transfer functions for oleic, palmitoleic, and linoleic acids. Transfer *curves* are normalized to the maximum integral of the $H_{allylic}$ peak for each fatty acid. **b** H_{methyl} to $H_{allylic}$ transfer functions for oleic, palmitoleic, and linoleic acids as well as those for the H_β to H_{methyl} transfer in saturated fatty acids to act as a length standard

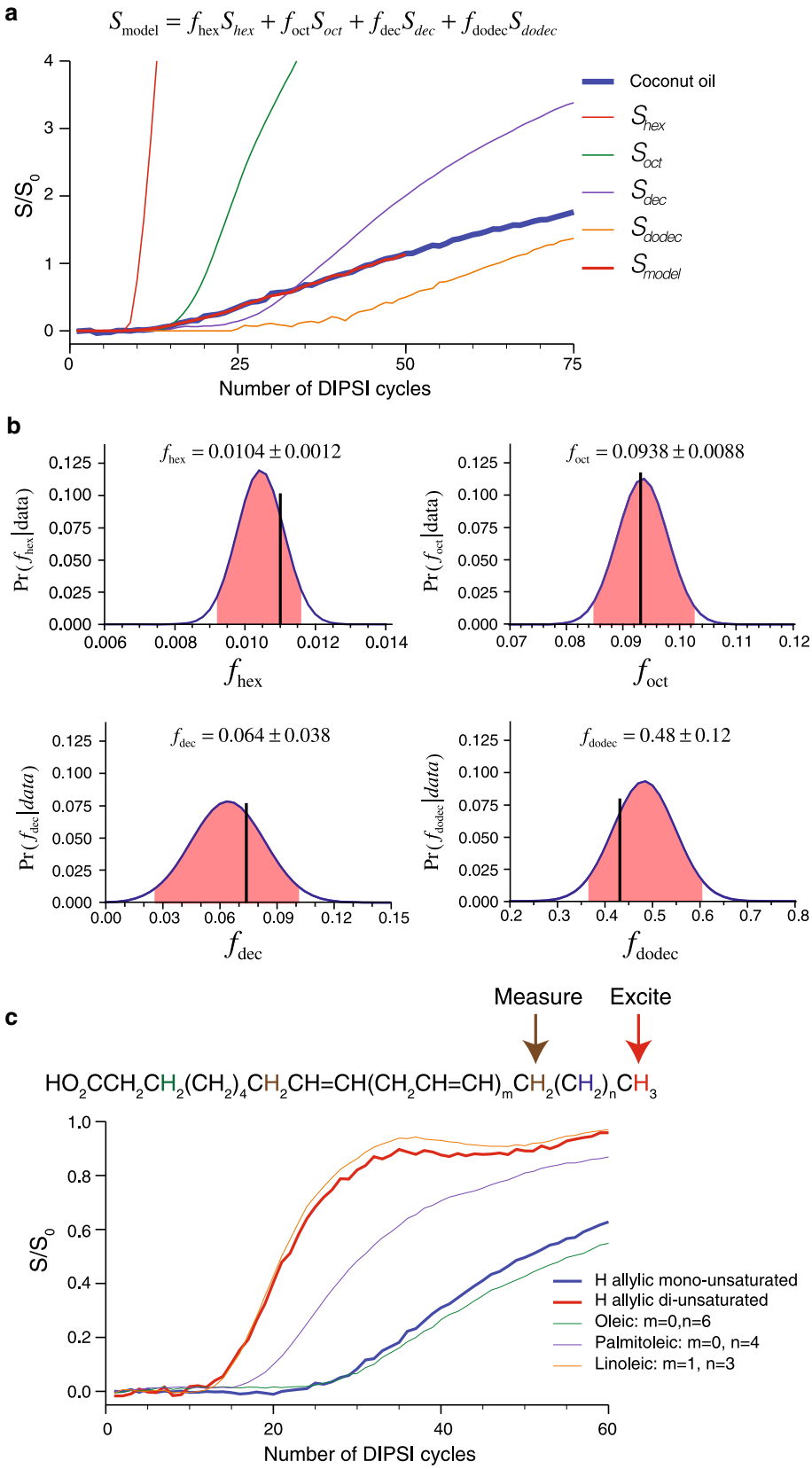

Fig. 4 ALCHIM of coconut oil. **a** H_β to H_{methyl} transfer function of coconut oil as well as the best fit model and those of hexanoic, octanoic, decanoic, and dodecanoic acids. **b** Probability distributions of the fatty acid fractions determined from modeling of the data. *Pink* regions are 95 % confidence intervals while the *vertical black lines* are the values determined by GC. **c** H_{methyl} to $H_{allylic}$ transfer function of coconut oil as well as oleic, palmitoleic, and linoleic acids. These data are normalized to the maximum transfer in each sample

four fractions given the data. The shaded pink regions give the 95 % confidence intervals of fractions: 1.04 ± 0.12, 9.38 ± 0.88, 6.4 ± 3.8, and 48 ± 12 % for hexanoic, octanoic, decanoic, and dodecanoic acids, respectively. The values for the fractions determined by GC and supplied by Supelco upon purchase (Online Resource) were 1.1, 9.3, 6.7, and 43.5 %. Thus, this method managed to accurately determine the fractions of the first 4 saturated fatty acids in this complex natural mixture.

The allylic peaks of the mixture were also analyzed after H_{methyl} excitation. As the allylic peaks from mono- and di-unsaturated fats are resolved in the 1D ^1H spectra (Online Resource), they can be monitored separately in the ALCHIM experiment. Figure 4c shows the transfer curves to the allylic protons for both mono- and di-unsaturated fatty acids. The transfer to $H_{allylic}$ monounsaturated overlays with that from oleic acid while the di-unsaturated overlays with linoleic acid. This immediately identifies the monounsaturated fat in coconut oil as ω-9 while the di-unsaturated fat is ω-6. By exciting at H_β and monitoring the two allylic peaks, it can be shown that the unsaturated fats are both Δ-9 fatty acids positively identifying them as linoleic and oleic acids.

FAME-RM2

FAME-RM2 is an analytical reference standard meant to mimic the fat distribution of hemp seed, linseed, perilla, and rubberseed oils. It contains methyl esters of oleic, linoleic, linolenic, palmitic, and stearic acid at weight percentages of 18.0, 36.0, 34.0, 7.0, and 5.0 % respectively. The ^1H spectra of FAME-RM2 and of representative unsaturated fatty acids are shown in the Online Resources. The chemical shift of the methyl protons in ω-3 PUFAs are shifted to 0.977 ppm while those for ω-6/ω-7/ω-9 unsaturated fatty acids and saturated fatty acids are observed near 0.885 ppm (Online Resources 1), allowing the ω-3 FAME methyl α-linolenate to be distinguished in this sample from the others (AOCS 2014). ALCHIM experiments performed on FAME-RM2 dissolved in $CDCl_3$ are shown in Fig. 5a, b. In these experiments the methyl peak at 0.885 ppm was selectively excited and the allylic peak was integrated as a function of the number of DIPSI cycles applied (Fig. 5a). This transfer curve was fit to a model assuming that the transfer curve is a linear combination of those from linoleic (ω-6), palmitoleic (ω-7), and oleic (ω-9) acids. Figure 5a shows the measured transfer curve of FAME-RM2 as well as those for the assumed constituents and the best-fit model. Figure 5b shows the probability distributions and 95 % confidence intervals for the unsaturated fatty acid fractions given the data. This sample was found to contain 13.0 ± 3.5 % oleic acid, less than 1.3 % palmitoleic acid, and 31.3 ± 0.52 % linoleic acid. GC analysis from the supplier gave the values as 18 % oleic acid, 0 % palmitoleic acid, and 36 % linoleic acid. These data show correctly that palmitoleic acid is not present in significant quantities in the sample. Oleic and linoleic acids are both underestimated by about 5 %.

Neutral fats extracted from mouse adipose tissue

ALCHIM experiments performed on neutral fats extracted from mouse adipose tissue and dissolved in deuterated chloroform are shown in Fig. 6a–c. ^1H 1D spectrum indicates that these neutral fats are triglycerides containing about 74 % unsaturated and 26 % saturated fatty acids. From the integrals of the allylic peaks, the amounts of mono- and di-unsaturated fatty acids are about equal (integral ratio 0.92). Figure 6a shows the transfer curves from H_{methyl} to $H_{allylic}$ of the monounsaturated fatty acids, which follows neither the reference curves for palmitoleic or oleic acids. The observed curve is modeled as a linear combination of these fatty acids and the probability distributions for the fitted fractions are shown in Fig. 6b. Neutral fats from mouse adipose tissue is found to contain 5.02 ± 0.11 % palmitoleic acid and 22.7 ± 0.51 % oleic acid. Figure 6c shows the curve from H_{methyl} to $H_{allylic}$ of the di-unsaturated fatty acids, which overlaps with that from linoleic acid indicating that this is an ω-6 di-unsaturated fatty acid. The H_β to $H_{allylic}$ of di-unsaturated fatty acid confirms that the observed acid is linoleic. Transfer from H_β to H_{methyl} was very inefficient, suggesting that the saturated fatty acids were long chain with the number of carbons greater than 14.

Mouse adipocytes

As a final test of the generality of the method, whole mouse adipocytes were isolated and placed in an NMR tube and the ALCHIM experiment performed. Figure 6d shows the results of the H_{methyl} to $H_{allylic}$ transfer as well as reference transfer curves from deuterated chloroform solution of oleic, palmitoleic, and linoleic acids. The peaks from the whole adipocyte sample were much broader than that seen from solutions, but the different sites in the fatty acids could still be distinguished (Online Resource Figure 6); however, it was not possible to distinguish the allyic peaks from mono- and di-unsaturated fatty acids. Figure 6d then shows the integral of both these contributions as a function of the mixing cycles. Figure 6d is not a fit, but simply an overlay. Since rise in the transfer curve for allylic protons in both linoleic acid and whole adipocytes occurs in the same range of DIPSI mixing cycles, linoleic acid must be present in the whole adipocytes. The presence of oleic acid is not seen because of the lack of resolution of the allylic

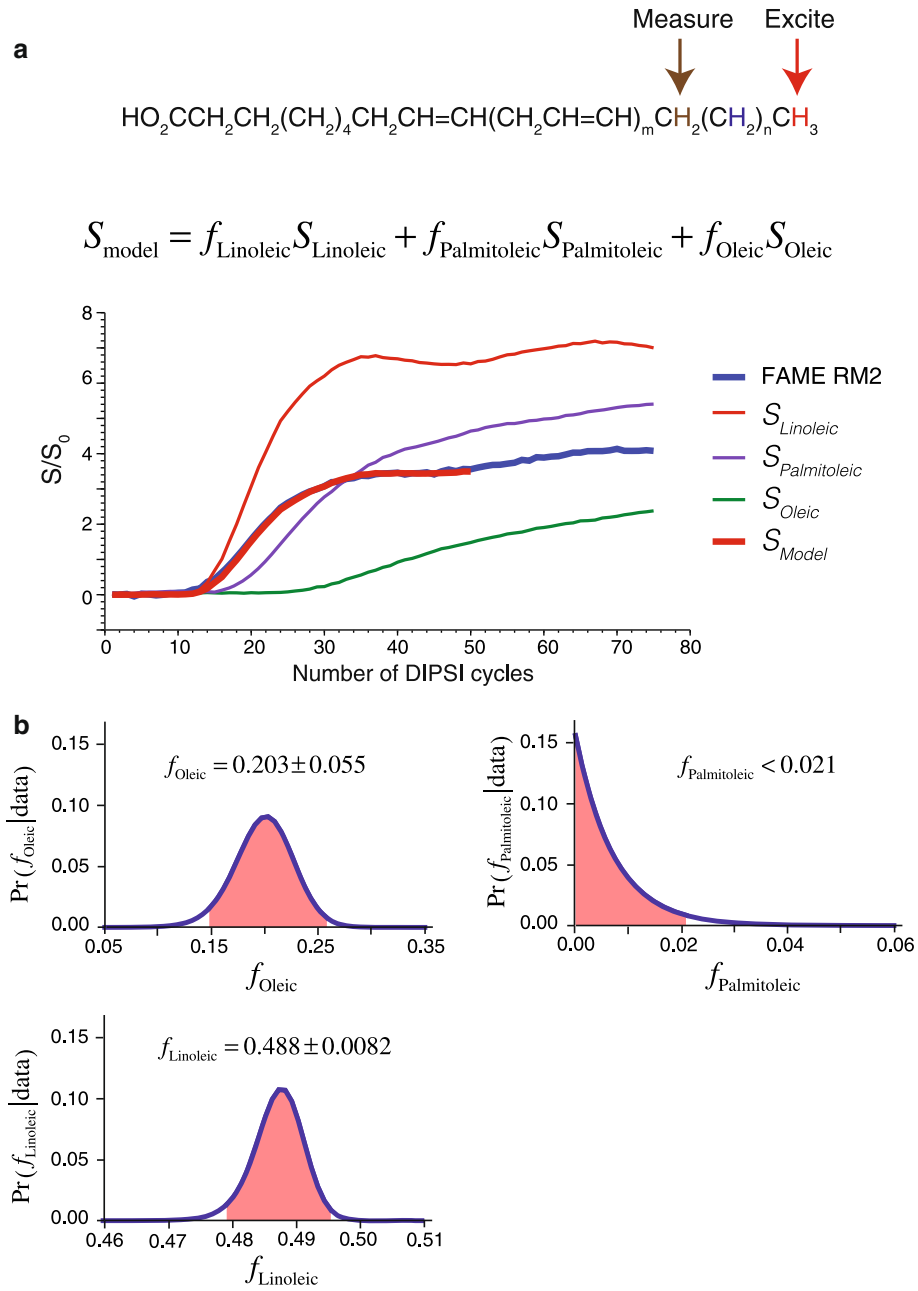

Fig. 5 ALCHIM of FAME analytical reference mix. **a** Hmethyl-1 (0.885 ppm) to Hallylic transfer function of FAME-RM2 as well as the best fit model and those of linoleic, palmitoleic, and oleic acids. **b** Probability distributions of the unsaturated fatty acid distributions determined from the data modeling. *Pink* regions are 95 % confidence intervals

peaks of mono- and di-unsaturated fatty acids and the much less sensitive long range transfer in oleic acid.

Discussion

ALCHIM in saturated and unsaturated fatty acids

Figure 1c shows the ALCHIM transfer curves for a series of saturated fatty acids from 6 to 12 carbons long. Several trends in the data are immediately obvious. First, the number of DIPSI cycles to transfer magnetization from H_β to H_{methyl} depends linearly on the number of carbon atoms separating the two positions. This is shown in Fig. 1d, where the maximum slope is plotted against the number of carbons in the fatty acid chain. Second, the transferred peak intensity decreases as the chain length increases as the isotropic mixing sequence distributes the initial magnetization over all spins in the chain. This suggests that the longer saturated fatty acids will be less sensitive than shorter in this experiment. This will ultimately limit this technique's ability to measure long chain ($C > 12$) and very long chain ($C > 22$) saturated fatty acids. In our hands, fatty acids chains for C12:0 and C14:0 were

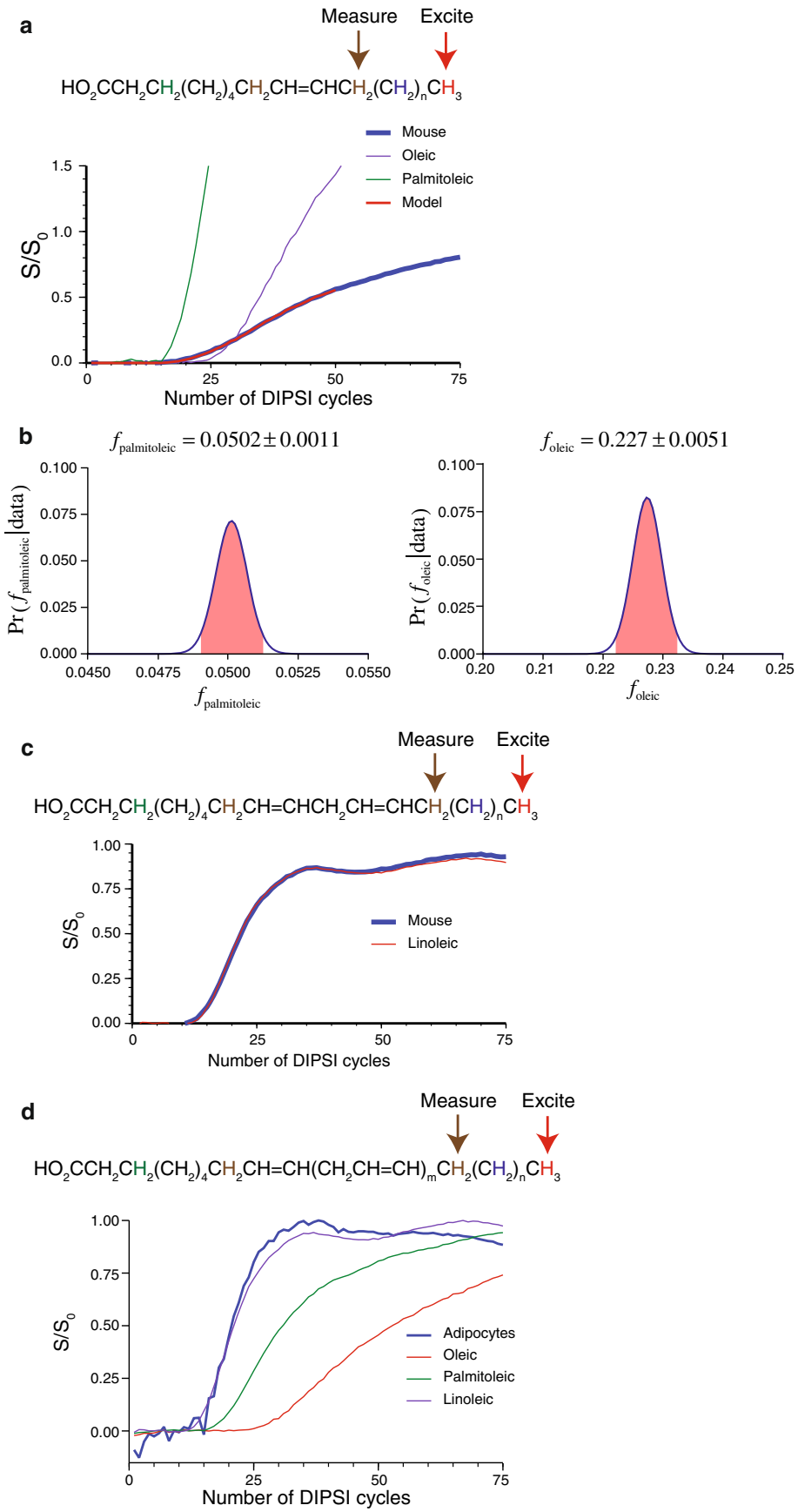

Fig. 6 ALCHIM of neutral mouse lipids. **a** H_{methyl} to mono-unsaturated $H_{allylic}$ transfer function of neutral mouse lipids. Also shown are the transfer functions of oleic and palmitoleic acids and the best fit model assuming the observed transfer function is their linear combination. **b** Probability distributions of the fatty acid fractions determined from modeling of the data. *Pink* regions are 95 % confidence intervals. **c** H_{methyl} to di-unsaturated $H_{allylic}$ transfer function in mouse fat as well as transfer functions of linoleic acid. **d** H_{methyl} to $H_{allylic}$ transfer function in mouse adipocytes as well reference transfer functions. Transfer functions were normalized to maximum

measurable but longer than that the signal-to-noise ratio was significantly degraded. An additional issue with the longer chain fatty acids is that the slope of the methyl intensity with the number of DIPSI cycles decreases as the chain length increases, making that rise more difficult to detect. Short fatty acids also show stronger oscillations in the methyl intensity. As the chain length becomes progressively longer, more frequencies are present leading to smoother transfer behavior. These oscillations do act as distinct fingerprints of the short fatty acids. These behaviors confirm the predictions of the simple chain model and demonstrate that fatty acid chain length can be measured with this technique.

By appropriately choosing the excitation and detection sites in the fatty acid, it is possible to make their identification. This is possible due to the linear behavior of the transfer as well as NMR's ability to site selectively excite and detect. Thus to identify saturated fatty acids, it is sufficient to excite at H_{β} and detect at H_{methyl}. In unsaturated fatty acids, two transfer curves must be measured so that the position of the unsaturation can be specified from both ends of the fatty acid chain. In this case, excitation is made at the H_{β} and the H_{methyl} with detection at $H_{allylic}$. As the $H_{allylic}$ resonances in mono- and di-unsaturated fatty acid occur at slightly different shifts, 2.011 ppm versus 2.048 ppm, respectively, two component mixtures of these unsaturated fatty acids can be easily identified using this strategy; however, we have also shown that fitting the integrals of the entire allylic region also allows identification of different unsaturated fatty acids. Vinylic protons, which only occur in multiply unsaturated fatty acids can also be probed.

ALCHIM in mixtures

In cases where the chemical shift does not resolve different components of a mixture, ALCHIM still permits analysis. Figure 2 demonstrates that the observed transfer curves are simple linear combinations of the components. This feature allowed the identification and quantification of the four lowest molecular mass saturated fatty acids in coconut oil, Fig. 4a, b. The probability distributions for the determined fractions of these fatty acids show that the method is most sensitive to the shorter lipids. This is demonstrated by the increased relative error in the determined fraction for the longer chain fatty acids. Two factors lead to this decreased precision: the longer chain fatty acids require deconvolution of the transfer functions of those shorter and the longer fatty acids have a smaller effect on the observed peak intensity as pointed out earlier. Despite this limitation, we have demonstrated that ALCHIM can successfully measure mixtures of saturated fatty acids with chain length 12 carbons or less. In unsaturated fatty acids, longer lipids can be probed because transfer down the entire chain is unnecessary as detection occurs in the center of the chain at the allylic proton.

While most of the samples analyzed in this paper were dissolved in deuterated chloroform, we have demonstrated that even whole adipocytes can be probed with this method. The linewidths of the ^{1}H resonances in the adipocyte sample were much broader than those in the chloroform; however, resolution was sufficient to selectively excite and detect the relevant sites in the lipid sidechains. This did lead to additional complexity in probing unsaturated fatty acids as the allylic peaks from mono- and di-unsaturated fatty acids were now unresolved. It was found that linoleic acid made the major contribution to the H_{methyl} to $H_{allylic}$ transfer curve because linoleic acid has 3 less carbons between these sites than oleic acid, the other major component identified in the extracted samples. This once again emphasizes that ALCHIM is most sensitive to shorter transfers in mixtures.

The analysis of the FAME-RM2 analytical standard sample demonstrated the power of this method in analyzing a complex mixture using a combination of quantitative ^{1}H NMR spectroscopy and ALCHIM. From the integrals of the methyl and allylic peaks, the sample was determined to contain 87.9 % unsaturated fatty acids and 12.1 % saturated fatty acids (actual 87.5 % unsaturated, 12.5 % saturated.) Of the unsaturated fatty acids, 35.8 % is ω-3 unsaturated (actual 34.0 %) while ω-6 and ω-9 are 31.3 ± 0.52 % (actual 36 %) and 13.0 ± 3.5 % (actual 18 %), respectively. These values are all within 5 % of the actual values.

Fat distributions in mouse adipose tissue

Agreeing with previous gas chromatography-based studies (Tallman and Taylor 2003; Li et al. 2010), oleic and palmitoleic acid were the principal mono-unsaturated lipids identified in mouse adipose tissue using ALCHIM. Both Li et al. and Tallman et al. reported roughly 4.5 and 30 % for palmitoleic and oleic acid, respectively, in mouse adipose tissue. These studies also identified linoleic acid as the major PUFA, with its contribution about 35 % of the analyzed lipids. By NMR, we observed similar numbers with roughly 5, 23, and 30 % for palmitoleic, oleic, and linoleic acid, respectively. While small variance exists between the published GC and ALCHIM results, this is likely due to differences in rodent diets, lipid extraction method, and type of mouse used. Our study used exclusively CD-1 female mice while the previous GC-based analyses used all male C57BL6 mice. Despite these differences, adipocyte-extracted lipid species and their concentrations identified using ALCHIM generally agree with GC based measures.

We have demonstrated a new use of the classic TOCSY technique for probing the structure of fats by magnetic resonance. This selective TOCSY experiment measures the aliphatic chain length by the dynamics of the magnetization transfer between the sites of interest. By comparing to a library of transfer functions, ALCHIM provides both qualitative and quantitative information about the composition of complex lipid samples and when combined with existing methods provides a much more complete understanding of these systems. For instance, it can distinguish ω-6 and ω-9 fatty acids in a mixture. Admittedly, ALCHIM transfer functions need to be measured on each instrument under the conditions used, but ALCHIM can be expected to work even at the highest fields as the chemical shift range of fatty acids is limited to the range 0.85 to 5.5 ppm. On a 1 GHz magnet this is only 4,700 Hz, which can be easily recoupled using a DIPSI-2 sequence with an rf field strength of 5,000 Hz. A great advantage of this method is that it works under many different conditions: from low viscosity solutions to high viscosity suspensions of whole cells. Since the sequence relies on selective excitation, contaminants are of little concern as long as they do not overlap with both the excited and detected peaks even if they are within the excitation bandwidth of the selective pulse. When combined with High-Resolution Magic Angle Spinning (HRMAS), this method will allow direct identification of fats in complex tissue samples. The method will be applicable to many systems in addition to those studied here, including micelles, bicelles, lipid nanoparticles, and nanodisks.

Acknowledgments We would like to thank Stephen Meredith and Shohei Koide for useful discussion and comments. This work was supported by NIH R01-CA148814 (S.D. Conzen), DOD predoctoral fellowship W81XWH-11-1-014901 (P.A. Volden) and by the Biological Sciences Division, the Office of Shared Research Facilities, and the Department of Biochemistry and Molecular Biology (J.R. Sachleben) at the University of Chicago.

References

AOAC (1995) Official methods of analysis of AOAC international. AOAC International, Gaithersburg, MD

AOCS Lipid Library (2014) http://lipidlibrary.aocs.org/

Boslem E, Weir JM, MacIntosh G, Sue N, Cantley J, Meikle PJ, Biden TJ (2013) Alteration of endoplasmic reticulum lipid rafts contributes to lipotoxicity in pancreatic β-cells. J Biol Chem 288:26569–26582

Braunschweiler L, Ernst RR (1983) Coherence transfer by isotropic mixing: application to proton correlation spectroscopy. J Magn Reson 53:521–528

Camont L, Lhomme M, Rached F, Goff WL, Nègre-Salvayre A, Salvayre R, Calzada C, Lagarde M, Chapman MJ, Kontush A (2013) Small, dense high-density lipoprotein-3 particles are enriched in negatively charged phospholipids: relevance to cellular cholesterol efflux, antioxidative, antithrombotic, anti-inflammatory, and antiapoptotic functionalities. Arterioscler Thromb Vasc Biol 33:2715–2723

Casado B, Affolter M, Kussmann M (2009) OMICS-rooted studies of milk proteins, oligosaccharides and lipids. J Proteomics 73:196–208

Didangelos A, Stegemann C, Mayr M (2012) The-omics era: proteomics and lipidomics in vascular research. Atherosclerosis 221:12–17

Ernst RR, Bodenhausen G, Wokaun A (1990) Principles of nuclear magnetic resonance in one and two dimensions. International series of monographs on chemistry. Clarendon Press, Oxford

Fedor D, Kelley DS (2009) Prevention of insulin resistance by n-3 polyunsaturated fatty acids. Curr Opin Clin Nutr Metab Care 12:138–146

Gelman A, Carlin JB, Stern HS, Rubin DB (2004) Bayesian data analysis, 2nd edn. CRC Press, Boca Raton

Gonzalez-Covarrubias V (2013) Lipidomics in longevity and healthy aging. Biogerontology 14:663–672

Gross RW, Han X (2007) Lipidomics in diabetes and the metabolic syndrome. Methods Enzymol 433:73–90

Guillén MD, Ruiz A (2001) High resolution 1H nuclear magnetic resonance in the study of edible oils and fats. Trends Food Sci Tech 12:328–338

Kamphorst JJ, Cross JR, Fan J, de E Stanchina, Mathew R, White EP, Thompson CB, Rabinowitz JD (2013) Hypoxic and Ras-transformed cells support growth by scavenging unsaturated fatty acids from lysophospholipids. Proc Natl Acad Sci USA 110:8882–8887

Kessler H, Oschkinat H, Griesinger C, Bermel W (1986) Transformation of homonuclear two-dimensional NMR techniques into one-dimensional techniques using Gaussian pulses. J Magn Reson 70:106–133

Kien CL, Bunn JY, Poynter ME, Stevens R, Bain J, Ikayeva O, Fukagawa NK, Champagne CM, Crain KI, Koves TR, Muoio DM (2013) A lipidomics analysis of the relationship between dietary fatty acid composition and insulin sensitivity in young adults. Diabetes 62:1054–1063

Kontush A, Chapman MJ (2010) Lipidomics as a tool for the study of lipoprotein metabolism. Curr Atheroscler Rep 12:194–201

Kwan HY, Hu YM, Chan CL, Cao HH, Cheng CY, Pan SY, Tse KW, Wu YC, Yu ZL, Fong WF (2013) Lipidomics identification of metabolic biomarkers in chemically induced hypertriglyceridemic mice. J Proteome Res 12:1387–1398

Li M, Fu W, Li X-A (2010) Differential fatty acid profile in adipose and non-adipose tissues in obese mice. Int J Clin Exp Med 3(4):303–307

Longobardi F, Sacco D, Casiello G, Ventrella A, Contessa A, Sacco A (2012) Garganica kid goat meat: physico-chemical characterization and nutritional impacts. J Food Compost Anal 28(2):107–113

Meikle PJ, Christopher MJ (2011) Lipidomics is providing new insight into the metabolic syndrome and its sequelae. Curr Opin Lipidol 22:210–215

Merched AJ, Chan L (2013) Nutrigenetics and nutrigenomics of atherosclerosis. Curr Atheroscler Rep 15. doi:10.1007/s11883-013-0328-6

O'Donnell VB, Maskrey B, Taylor GW (2009) Eicosanoids: generation and detection in mammalian cells. In: Larijani B et al. (eds) Lipid signaling protocols. Humana Press, Totowa, N.J., pp 5–23. doi:10.1007/978-1-60327-115-8_1

Rasmiena AA, Ng TW, Meikle PJ (2013) Metabolomics and ischaemic heart disease. Clin Sci 124:289–306

Riccardi G, Giacco R, Rivellese AA (2004) Dietary fat, insulin sensitivity and the metabolic syndrome. Clin Nutr 23:447–456

Rule GS, Hitchens TK (2006) Fundamentals of protein NMR spectroscopy. Focus on structural biology. Springer, Dordrecht

Sachleben JR (2006) Bayesian and information theory analysis of MAS sideband patterns in spin 1/2 systems. J Magn Reson 183:123–133

Sbihi HM, Nehdi IA, Al-Resayes SI (2013) Characterization of Hachi (*Camelus dromedarius*) fat extracted from the hump. Food Chem 139(1–4):649–654

Simonsen N, Pvt Veer, Strain JJ, Martin-Moreno JM, Huttunen JK, Navajas JFC, Martin BC, Thamm M, Kardinaal AFM, Kok FJ, Kohlmeier L (1998) Adipose tissue omega-3 and omega-6 fatty acid content and breast cancer in the EURAMIC study. Am J Epidemiol 147:342–352

Sivia DS (1996) Data analysis: a bayesian tutorial. Clarendon Press, Oxford

Ståhlman M, Pham HT, Adiels M, Mitchell TW, Blanksby SJ, Fagerberg B, Ekroos K, Borén J (2012) Clinical dyslipidaemia is associated with changes in the lipid composition and inflammatory properties of apolipoprotein-B-containing lipoproteins from women with type 2 diabetes. Diabetologia 55:1156–1166

Stonehouse J, Adell P, Keeler J, Shaka AJ (1994) Ultrahigh-quality NOE spectra. J Am Chem Soc 116:6037–6038

Stott K, Stonehouse J, Keeler J, Hwang TL, Shaka AJ (1995) Excitation sculpting in high-resolution nuclear magnetic resonance spectroscopy: application to selective NOE experiments. J Am Chem Soc 117:4199–4200

Tallman DL, Taylor CG (2003) Effects of dietary fat and zinc on adiposity, serum leptin, and adipose fatty acid composition in C57BL/6 J mice. J Nutr Biochem 14:17–23

Thiebaut ACM, Chajes V, Gerber M, Boutron-Rualt MC, Joulin V, Lenoir G, Berrino F, Riboli E, Benichou J, Clavel-Chapelon F (2009) Dietary intakes of omega-6 and omega-3 polyunsaturated fatty acids and the risk of breast cancer. Int J Cancer 124:924–931

Thrippleton MJ, Keeler J (2003) Elimination of zero-quantum interference in two-dimensional NMR spectra. Angew Chem Int Ed 42:3938–3941

Van QN, Shaka AJ (1998) Improved cross peak detection in two-dimensional proton NMR spectra using excitation sculpting. J Magn Reson 132:154–158

Watson AD (2006) Thematic review series: systems biology approaches to metabolic and cardiovascular disorders. J Lipid Res 47:2101–2111